Fourth International Conference on
Applications of Statistics and Probability in Soil and Structural Engineering.
Università di Firenze (Italy) 1983, Pitagora Editrice.

PROBABILISTIC PROBLEMS IN PREDICTION OF CREEP AND SHRINKAGE EFFECTS IN STRUCTURES

Zdeněk P. Bažant
Professor of Civil Engineering and Director
Center for Concrete and Geomaterials
Northwestern University
Evanston, Illinois 60201, U.S.A.

Abstract. - A review of some recent results obtained at Northwestern University in probabilistic analysis of creep and shrinkage effects in structures is presented. After summarizing results of extensive statistical studies of test data existing in the literature, a Bayesian prediction method is outlined. The prior probability distribution based on test data from the literature is updated using limited test data for a given concrete to yield a posterior probability distribution to be used in design with the given concrete. Subsequently, the effects of random fluctuations of environmental humidity or temperature upon shrinkage and creep are analyzed. The spectral method is generalized for this purpose to linear aging systems. Finally, other sources of randomness, including randomness of creep increments due to the creep mechanism, are discussed.

Introduction

Creep and shrinkage appears to be the most uncertain phenomenon in the design of concrete structures. The statistical variability of creep and shrinkage is far greater than that of concrete strength, yet statistical methods have been so far well developed only for the latter. Part of the reason is that the problem of creep and shrinkage is more difficult, and part of the reason is that the consequences of a substantial error in creep and shrinkage prediction are generally less disastrous than they are for errors in strength. Creep buckling excepted, they do not cause structural collapse but merely put the structure out of service, as a result of excessive cracking (which causes, e.g., reinforcement corrosion) or excessive deflections. Nevertheless, for reasons of economy, it is imperative to improve the prediction of the creep and shrinkage effects in structures and, in particular, develop a method of design for extreme rather than average creep predictions.

Practical probabilistic analysis of concrete creep and shrinkage has recently been rendered meaningful by extraction of an extensive body of statistical information from the literature; see Ref. 1 and 2, in which test data for 80 different concretes from various laboratories throughout the world, consisting of over 800 experimental curves and over 10,000 data points, have been analyzed statistically and organized in a computerized data bank [3]. It has been shown, that if no measurements for a given concrete are made, the uncertainty of its creep and shrinkage prediction on the basis of the chosen concrete mix parameters and the chosen design strength is enormous. For all the data considered, it was determined [2] that, on the whole, the prediction errors that are exceeded with a 10% probability (90% confidence limits) are, for the best known practical prediction models, as follows:

BP Model [1]: $\omega_{90} = 31\%$

ACI - 1971 Model [4, 5]: $\omega_{90} = 63\%$

CEB-FIP - 1978 Model [6]: $\omega_{90} = 76\%$

The first of these models is to a greater extent than the others based on physical considerations and is applicable over a much wider range of con-

ditions. However, it is relatively complicated. The second model is much simpler, and still represents probably the optimum prediction method at its degree of simplicity. The question of simplicity should, however, be viewed in a proper perspective. The mentality of a stuctural designer is opposite to that of a materials engineer. He does not mind to spend weeks or months on stress analysis of structures, but considers it objectionable if the determination of material properties that enter his analysis takes more than 10 minutes. Yet, the material properties are, in case of creep and shrinkage, a much greater source of error than any simplifications of analysis. The attitude of a materials engineer, who would prefer spending weeks on determining his material properties and then 10 minutes on structural analysis would probably lead to a smaller error. In any event, structural engineers ought to devote, in the case of creep and shrinkage analysis, at least the same time to the determination of creep and shrinkage properties as they do to stress calculations [2].

From the physical point of view, one can distinguish the following four causes of randomness in concrete creep and shrinkage:

1. Randomness due to uncontrollable variations in material properties.
2. Randomness due to variations in the environment (weather).
3. Randomness of the creep or shrinkage increments due to the statistical nature of the physical mechanism itself [8].
4. Measurement error.

The first of these causes of uncertainty is by far the worst. It may be, however, largely eliminated by carrying out a few limited measurements and applying the Bayesian analysis which follows. Among the remaining causes of uncertainty, the second one is worst. It will be also addressed here. If the environment is perfectly controlled in the laboratory, or

if a mass concrete with hardly any communication with the environment is considered, the second cause of uncertainty is also largely eliminated. Then the randomness of the creep mechanism per se remains as the remaining principal cause of uncertainty [8, 9]. As for the measurement error, it represents an uncertainty that is not "felt" by the structure, but only by the observer. Therefore, this error should not be included in the creep and shrinkage prediction models for design, and must be eliminated from the measured data.

The purpose of the present lecture is to summarize and review several recent studies carried out at Northwestern University in collaboration with J. C. Chern, T. S. Wang, T. Tsubaki, L. Panula, E. Cinlar, E. Osman, and H. Madsen. No claims for an exhaustive coverage of the subject are made.

Statistics of Existing Data

Before undertaking statistical analysis, test data reported in the literature have to be first processed, for two reasons: (1) The data contain random fluctuations due to measurement error, and (2) The reading times have not been selected in a manner which would assure an unbiased weighting of successive time intervals. To eliminate these effects, it is most convenient and perhaps sufficient to smooth reported data points by hand, and then to take test data points for statistical analysis as the ordinates of the hand-smoothed curves at intervals spaced regularly in the logarithm of creep duration or shrinkage duration, normally two points per decade in the logarithmic scale.

The aforementioned approach to the processing of raw data from the literature has been followed in Refs. 1, 2, and 3. In a recent study at Northwestern University, S. Zebich [3] developed a fully computerized data bank involving essentially all the test data analyzed in Refs. 1 and 2.

In this data bank, the data points are organized in subscripted arrays, in which the first subscript refers to the number of the data point on the creep curve, the second subscript to the number of the creep curve within a certain data set, and the third subscript to the number of the data set. Another integer array defines the number of all data points on each creep curve, and the number of all curves in a given data set, and finally the number of all data sets in the data bank. Two data banks were generated; one for the points at properly spaced time intervals from the hand-smoothed data curves, and one for the unprocessed original data as reported. This data bank tremendously reduces the labor in extracting various statistics from the data and carrying out statistical analysis.

The analysis in Ref. 1 and 2 established the statistics (principally, the coefficient of variation) of the collection of deviations of hand-smoothed data from the prediction formulas for the compliance function and for the shrinkage strain. Statistically a more fundamental approach would be to analyze the variability of the parameters of the prediction formulas and use it to determine the variation of characteristics such as the coefficient of variation with the independent variables such as load duration or age at loading. Such an approach is, however, rather difficult because of the nonlinearity of the prediction formulas for the compliance function and the shrinkage strain. To be able to carry out an anlysis of this type, one needs to transform the prediction formulas into a linear form to which the standard linear regression analysis could be applied. This appears to be possible, and has been done by Zebich [3]. We summarize briefly some of the results.

We try to transform the prediction formula for creep on shrinkage to the linear form

$$y = a + bx + e \tag{1}$$

in which x and y are the transformed independent and dependent variables, b is the slope, a is the y-intercept, and e is the error. The transformation is such that for a perfect model b = 1 and a = 0.

Consider now basic creep, i.e., the creep at constant water content. The double power law for basic creep [1, 10] may be transformed to the following form:

$$y = E_0\, J(t,t') - 1 \quad (= \text{creep coefficient})$$
$$x = \left[1 + \phi_1 (t'^{-m} + \alpha)\ (t - t')^n\right] - 1 \tag{2}$$

in which J(t,t') = creep compliance (also called the creep function), representing the strain at age t caused in concrete by a constant uniaxial unit stress acting since age t'; E_0, ϕ_1, n, m, and α = material parameters defined in Ref. 10. The most important test data on basic creep, including those of L'Hermite et al., Hanson and Harboe (Shasta Dam, Ross Dam, and Canyon Ferry Dam), Browne (Wylfa vessel), Pirtz, et al. (Dworshak Dam), and Rostasy et al., have been subjected to regression analysis according to Eqs. 1-2. The resulting regression line (Eq. 1), as well as the 90% confidence limit for the mean prediction and for the individual data points are shown in Fig. 1a and the corresponding statistics are listed in Table 1, in which $\bar{x}$, $\bar{y}$ is the centroid of data points, s_x, s_y are the standard deviations of the data points, s_b is the standard deviation of slope b, $s_{y|x}$ is the standard deviation of the data points from the regression line, and r is the correlation coefficient.

There are other ways to transform the double power law to a linear form. One is

$$y = \log\left(\frac{J(t,t')\,E_0 - 1}{\phi_1\,(t^{-m} + \alpha)}\right), \qquad x = n \log\,(t - t') \tag{3}$$

and the regression analysis of the same data based on this equation is shown in Fig. 1b. The statistics are given in Table 1.

The ACI Model [4, 5, 10] can be transformed to a linear form as follows

$$y = E(t')\,J(t,t') - 1, \qquad x = C_u[1 + 10(t - t')^{-0.6}]^{-1} \tag{4}$$

in which $E(t')$ is the conventional elastic modulus at age t', and C_u is a material parameter calculated as a product of six other material parameters [4, 30]. Regression analysis of the same test data according to this equation is shown in Fig. 1c, and the statistics are again summarized in Table 1.

The CEB Model [6, 10] can be transformed to a linear form (Eq. 1) as follows

$$y = E_{28}J(t,t') - \frac{E_{28}}{E_c(t')} - \beta_a(t'), \quad x = \phi_d\beta_d(t,t') + \phi_f[\beta_f(t) - \beta_f(t')] \tag{5}$$

in which E_{28}, E_c, β_a, ϕ_d, β_d, ϕ_f, and β_f are material parameters and functions defined in Ref. 6. The results of the regression analysis on the same test data as before are shown for this model in Fig. 1d, and the corresponding statistics are listed in Table 1.

The BP model for shrinkage can be brought to a linear form in various ways, and one is

$$y = \log\left[\left(\frac{\varepsilon_\infty}{\varepsilon_{sh}}\right)^2 - 1\right], \qquad x = \log\frac{\tau_{sh}}{\hat{t}} \qquad (\hat{t} = t - t_0) \tag{6}$$

Similarly, for the ACI Model, the linearization may be achieved as follows

$$y = \log\left(\frac{0.0078}{\varepsilon_{sh}} - 1\right) \qquad x = \log 55 - \log \hat{t} \tag{7}$$

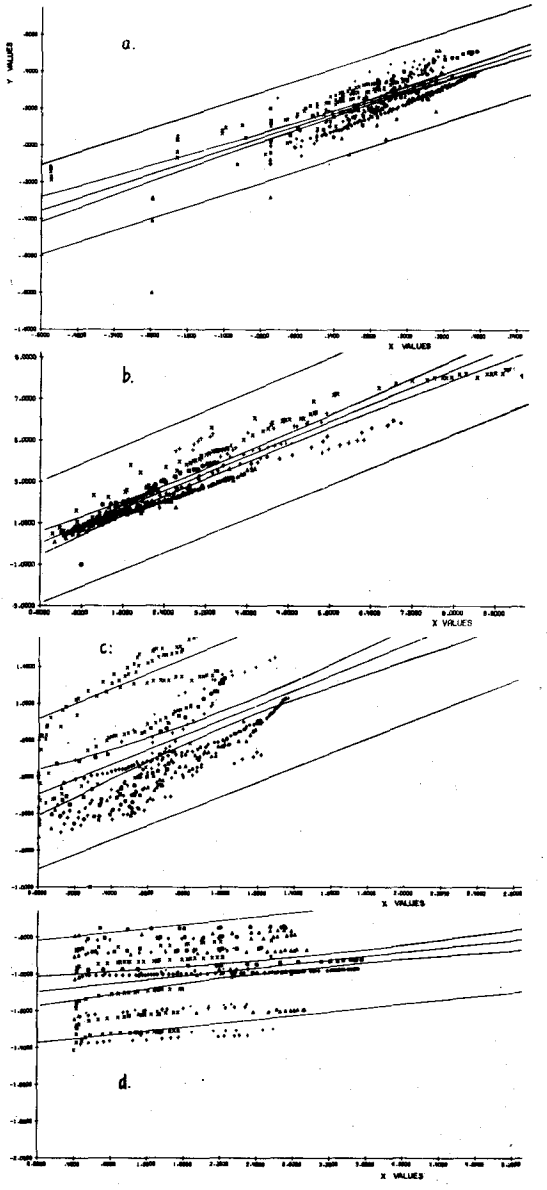

Fig. 1 - Zebich and Bažant's (1981) Comparison of Various Prediction Models for Basic Creep with Existing Test Data (see Text); a, b - BP Model (Eq. 2 and 3), c - ACI Model, d - CEB Model.

and for the CEB Model as follows

$$y = \log\left(\frac{\varepsilon_{sh}}{\varepsilon_{so}}\right) \quad , \qquad x = \log\left[\beta_s(t) - \beta_s(t_o)\right] \tag{8}$$

In these equations, ε_{sh} is the shrinkage strain, $\hat{t}$ is the duration of drying, t_o is the age at the start of drying, τ_{sh} is the shrinkage-square half time, proportional to effective thickness square, and ε_∞, τ_{sh}, ε_{so}, and β_s are material parameters and functions defined in Refs. 1, 2, 4, and 6. The most important shrinkage data from the literature, involving those on Hansen and Mattock, L'Hermite et al., Kesler et al., Troxel et al., and Keeton, have been used in regression analysis. The results for Eqs. 6, 7, and 8 are shown in Fig. 2a, b, c, respectively. The corresponding statistics are listed in Table 1.

A similar regression analysis can be carried out for creep during drying. In this case the linear regression plots are, however, less relavant, because creep at drying is a sum of a basic creep term and a drying creep term, both of which cannot be simultaneously varied in the regression plot. One of these terms must be fixed, and linear regression may then be carried out for the other term. For this reason, linear regression analysis of creep at drying for the BP Model would not be very informative.

The regression plots in Figs. 1 and 2 visually demonstrate the degree of agreement of the three models considered with the test data. Quantitatively, the degree of agreement is reflected best by the correlation coefficient r in Table 1; for perfect correlation r = 1, and the more r differs from 1, the poorer is the representation of test data. From these comparisons it appears, similarly to the conclusions of Ref. 1 and 2, that the BP Model agrees with test data clearly best.

The linear regression analyses in transformed variables must, however, be regarded with reservation since the transformation of variables

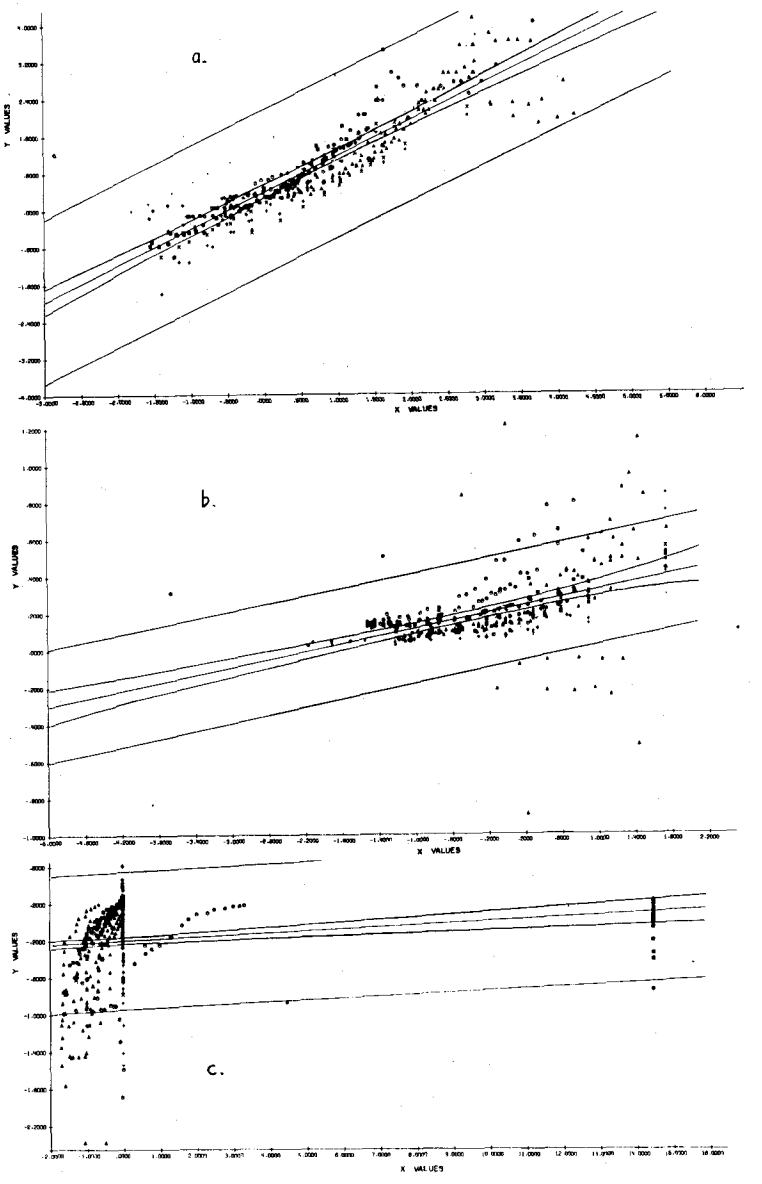

Fig. 2 - Zebich and Bažant's (1981) Comparison of Various Prediction Models for Shrinkage with Existing Test Data (see Text); a - BP Model (Eq. 6), b - ACI Model (Eq. 7), c - CEB Model (Eq. 8).

generally introduces bias, due to change of weighting of various time intervals as well as possible superimposition of a deterministic dependence (a blatant example of such bias was demonstrated for Ross' hyperbola in Ref. 7). Therefore, in spite of certain advantages mentioned before, the comparisons based on the regression plots in Figs. 1 and 2 should be considered secondary to the comparisons based directly on the deviations of the compliance values or the shrinkage values [1, 2].

Table 1 - Linear Regression Statistics of Test Data

Statistic	$\bar{x}$	$\bar{y}$	s_x	s_y	a	b	s_b	$s_{y\|x}$	r
a) Basic Creep									
BP									
Eq. 2, Fig. 1a	0.495	0.464	0.351	0.306	0.019	0.999	0.005	0.304	0.820
Eq. 3, Fig. 1b	2.559	2.739	1.713	1.916	0.180	1.062	0.003	1.92	0.933
ACI									
Eq. 4, Fig. 1c	0.630	0.520	0.335	0.521	-0.109	0.822	0.004	0.522	0.521
CEB									
Eq. 5, Fig. 1d	1.703	-1.004	0.862	0.173	-2.107	-0.458	0.005	0.173	0.265
b) Shrinkage									
BP									
Eq. 7, Fig. 2a	1.423	1.484	2.855	1.912	0.240	0.899	0.004	1.915	0.870
ACI									
Eq. 8, Fig. 2c	-0.495	0.166	1.973	0.185	0.411	0.044	0.005	0.185	0.479
CEB									
Eq. 9, Fig. 2c	-0.154	-0.204	0.866	0.459	-0.050	0.116	0.012	0.460	0.146

Bayesian Statistical Prediction

The uncertainty due to material parameters can be greatly reduced if at least some short-time data are measured for a given concrete at hand [2]. These data may be used to update the predictions of a model based on all the existing test data in the literature (prior information). A model

of this type has been developed by Chern and Bazant [11] at Northwestern University, and will be now outlined briefly.

Many creep prediction formulas, including the double power law, may be expressed in the linearized form

$$J(t,t') = q_1 x + q_2 + e \tag{9}$$

in which x may be called the reduced time, q_1, q_2 are material parameters, and e is the error. In particular, for the double power law one may set

$$q_1 = \phi_1/E_0, \quad q_2 = 1/E_0, \quad x = (t'^{-m} + \alpha)\ (t - t')^n \tag{10}$$

in which E_0, ϕ_1, m, n, and α are the material parameters in the double power law. Parameters m, n and α must be considered as fixed while parameters E_0 and ϕ_1 are random and may be expressed from the random basic material parameters q_1 and q_2.

Assume that the probability density distribution $f'(q_1, q_2)$ of the possible parameter values is known from prior experimental information on various concretes. This distrigution is called prior.

Now assume that, for a given concrete, certain compliance values J_j at some reduced times x_j (j = 1, 2,...N) have been measured. We wish to exploit this information to update the probability density distribution $f'(q_1, q_2)$ to obtain an improved, posterior probability density distribution $f"q_1, q_2)$. According to Bayes' theorem [12-17]:

$$f"(q_1, q_2) = k\ P(J_j|q_i)\ f'(q_1, q_2) \tag{11}$$

in which | denotes conditional probability, i.e., $P(J_j|q_i)$ is the probability of observing values J_j under the condition that the parameter values are q_i; and k is a normalizing constant which assures that the integral of $f"(q_1, q_2)$ over the entire two dimensional infinite domain be unity, i.e.,

$$k = \left[\int_{-\infty}^{\infty} \int_{-\infty}^{\infty} P(J_j|q_i)\ f'(q_1, q_2)\ dq_1\ dq_2 \right]^{-1} \tag{12}$$

The conditional probability $P(J_j|q_i)$ represents what is usually called the likelihood function.

Assuming, for the sake of simplicity, that the observed values $J_1, \ldots J_n$ are statistically independent of each other, we may set

$$P(J_j|q_i) = \prod_{j=1}^{N} f_j(J_j|q_1, q_2) \tag{13}$$

in which $f_j(J_j|q_i)$ is the probability density distribution of the random variable J_j given that the observed parameter values are q_1 and q_2. For one given concrete, parameters q_1, q_2 are fixed, and so the function $f_j\ (j_j|q_1, q_2)$ describes the scatter of J_j in one and the same concrete.

Although objections may be raised due to the physical impossibility of very large negative errors of J_j, we may assume, for the sake of simplicity, that the compliance values J_j for certain parameters values q_1, q_2 and a certain fixed reduced time x_j is a normal random variable with the mean $(q_1 x_j + q_2)$ and standard deviation σ, i.e.,

$$f_j(J_j|q_1, q_2) = \frac{1}{\sigma\sqrt{2\pi}} \exp\left[-\left(\frac{J_j - q_1 x_j - q_2}{\sigma} \right)^2 \right] \tag{14}$$

The standard deviation σ characterizes the given concrete for which measurements J_j were taken. If these are insufficient to determine σ realiably, one may use for σ a typical value for any similar concrete.

Assuming σ to be independent of x, we thus obtain the result

$$f''(q_1, q_2) = a_0 \exp\left[-\frac{1}{2} \sum_{j=1}^{N} \left(\frac{J_j - q_1 x_j - q_2}{\sigma} \right)^2 \right] f'(q_1, q_2),\quad a_0 = k\ \sigma\sqrt{2\pi}^{-N} \tag{15}$$

Thus, the posterior (updated) probability that the compliance J(x) at reduced time x will be less than some given value $\hat{J}$ may be determined as

$$P\ [J(x) < \hat{J}] = \int_{-\infty}^{\infty} \int_{-\infty}^{\infty} \Phi[y(q_1, q_2)]\ f''(q_1, q_2)\ d\ q_1\ d\ q_2 \tag{16}$$

in which

$$\Phi[y(q_1, q_2)] = P\ [J(x) < \hat{J}|q_1, q_2] = \frac{1}{\sigma\sqrt{2\pi}} \int_{-\infty}^{y} e^{-z^2/2\sigma^2}\ dz \tag{17}$$

where Φ represents the cummulative normal distribution function, and $y(q_1, q_2) = (\hat{J} - q_1\ x - q_2)\ /\sigma$.

Although again there exists objections in view of possible very large negative errors in J, we adopt for the prior distribution $f''(q_1, q_2)$ a normal distribution. Properly, a bivariate distribution with two variables q_1 and q_2 should be considered. Unfortunately, however, no statistical data are available for the scatter of parameters q_1 and q_2. The only data which are plentiful are those on the variability of J(x), from which one can determine the normal distribution

$$f\ [J(x)] = \frac{1}{\sigma_j(x)\sqrt{2\pi}} \exp\left[-\frac{1}{2} \left(\frac{\bar{J}(x) - J(x)}{\sigma'_J(x)} \right)^2 \right] \tag{18}$$

in which $\bar{J}$ is the mean of J, σ_J is the corresponding standard deviation. Now, if we substitute $J(x) = q_1\ x + q_2$, this distribution becomes a function of q_1 and q_2, and may be approximately treated as the desired prior distribution of the values of parameters q_1 and q_2:

$$f'\ (q_1, q_2) = \frac{1}{\sigma'_J\sqrt{2\pi}} \exp\left[-\frac{1}{2} \left(\frac{\bar{J}(x) - q_1\ x - q_2}{\sigma_J(x)} \right)^2 \right] \tag{19}$$

We have replaced here the standard deviation σ_J at any small x by the standard variation σ'_J at the centroid of all data, i.e., $\sigma'_J = \omega_J\ \bar{J}_0$ where

J_0 is the mean of all observed J-values. The standard deviation at x may be approximated as $\sigma_J(x) = \omega_J \bar{J}(x)$ where ω_J is the coefficient of variation of the prior data, for which extensive data exist (Table 3 of Ref. 1).

What remains is to integrate Eq. 16. This has to be done numerically, and caution is required. The shape of the integrant invariables q_1 and q_2 is so complicated that direct application of numerical integration formulas could not succeed. It is necessary to substitute new variables which would make numerical integration feasible. The posterior distribution has the general form

$$f''(q_1,q_2) = a_0 \exp\left[-(c_1 q_1^2 + c_2 q_2^2 + c_3 q_1 q_2 + c_4 q_1 + c_5 q_2 + c_6)\right] f'(q_1, q_2) \tag{20}$$

in which $c_1, c_2 \ldots c_6$ are certain constants. For the purpose of numerical integration one needs to introduce a linear substitution

$$u = a_1 q_1 + a_2 q_2 + q_3, \quad v = a_4 q_1 + a_5 q_2 + a_6 \tag{21}$$

with some coefficients $a_1, a_2, \ldots a_6$, such that the integrand in Eq. 20 is transformed to the form

$$f''(q_1, q_2)\, dq_1\, dq_2 = C_0\, e^{-u^2 - v^2}\, du\, dv \tag{22}$$

Such a transformation is derived in Ref. 11. In Eq. 22, numerical integration can be easily carried out using the Hermite-Gaussian formula.

In Fig. 3 we can see one of the examples calculated in detail in Ref. 11. This example concerns the concrete for which creep was measured by McDonald in Vicksburg (1975) [18]. First one should note the new prediction and the 90% probability band based on the prior information for all concretes [1]. We assume that only the first four data points of McDonald are known to us, and we try to use these four points to update the prior statistical information and compare the resulting prediction

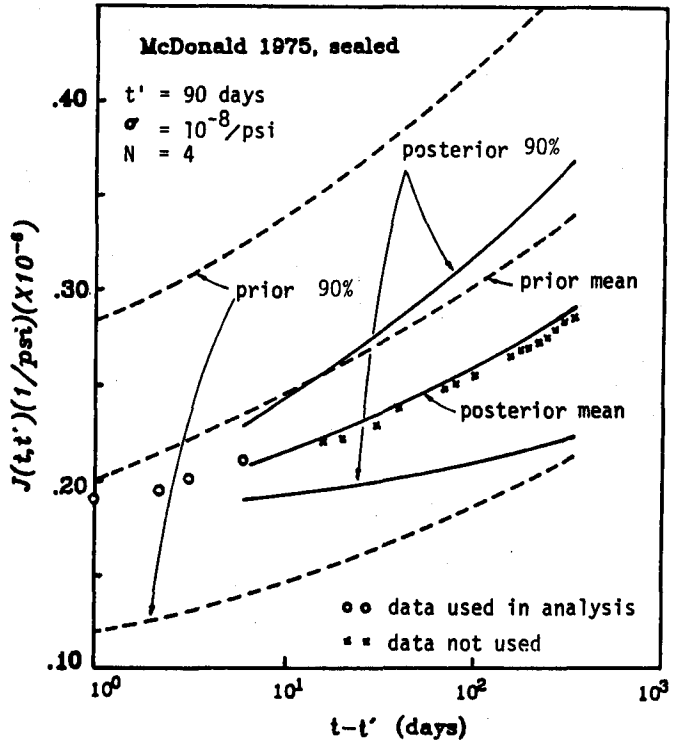

Fig. 3 - Example of Bayesian Prediction, Assuming only the First Four Points Measured by McDonald (1975) to be Known and the Rest of them Unknown.

to the remaining measurements of McDonald which have not been used in the analysis. The updated mean prediction and 90% probability band have been obtained by numerical integration of Eq. 16, with Eq. 17 and Eq. 22, and are also plotted in Fig. 3. Know that the updated, posterior mean prediction and 90% probability band are much closer to the remaining test data than the prior prediction, and the 90% probability band becomes much narrower than that for the prior information. The improvement in prediction, based only on several short time measurements, is indeed drastic. A similar improvement is documented by a number of other examples in Ref. 11.

A similar Bayesian analysis can be carried out for the BP formula for creep during drying as well as for shrinkage. The same analysis can be also carried out for various other creep formulas which can be brought to the linearized form of Eq. 9.

It should be noted that the foregoing Bayesian analysis is similar in various respects to the recent work of Tang [5] on Bayesian prediction of settlement of ocean oil platforms.

Spectral Analysis of the Effect of Random Environment

As discussed in the introduction, the second major source of uncertainty is the randomness of the fluctuations of environmental humidity, which produces random shrinkage stresses. A similar effect is due to random environmental temperature, and may be analyzed in the same manner. The magnitudes of the shrinkage stresses depends on the elastic modulus and is greatly offset by creep. The elastic as well as creep properties of concrete strongly depend on the age of concrete. This introduces a major complication for analysis, even if the stress-strain relation and the relation of shrinkage strain to pore humidity are linearized.

Generalizing an analysis of random thermal stresses in a nonaging viscoelastic thick-wall cylinder by Heller [19], the problem of shrinkage stresses caused by random environmental humidity was solved by Tsubaki and Bažant [20]. In view of aging, they used direct integration of impulse response functions. Subsequently it was shown, however, that a more efficient, general solution procedure is possible using the spectral approach [21]. The spectral method must however be generalized for the case of aging systems, which has apparently not been done so far. Based on Ref. 21, we will now explain this generalization briefly.

For a non-aging structure, the statistical characteristics of the response at a given point within the structure are those of the random time variation of the response at that point (ergodic property). However, this concept is inapplicable to an aging structure since the statistical characteristics of the response themselves very in time. For an aging structure, we must imagine an ensemble of a great number of identical structures (systems) exposed to different realizations of the input environment or loading) with the same statistical properties, while the age t_0 of the structure at the start of exposure or loading is the same for all these structures (Fig. 4a). Suppose we calculate the response value (e.g., the stress) at a certain point x and a certain age t ($t \geq t_0$) for all these structures, and then we consider the ensemble of all these response values (labeled as g_1, g_2, g_3,... in Fig. 4a). The statistical characteristics of the response that the engineer needs to know are those of this ensemble. He needs to know their dependence on spatial croordinates x, as well as t and t_0.

Calculation of the statistical characteristics at each x and t from all the values in this ensemble would, however, be too laborious. We need

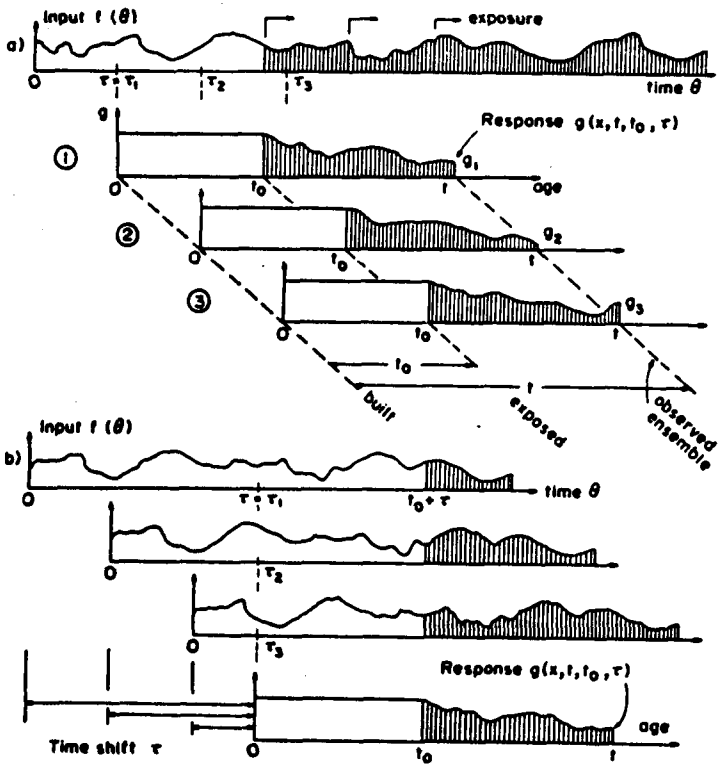

Fig. 4 - The Aging Aspect of Response of a Concrete Structure to Random Environment.

to introduce some continuous variable to arrange all the realizations of the input. This can be achieved by exploiting the fact that the input is a stationary random process. Instead of taking the statistics of all the responses (at x and t) for all realizations of the same input on various identical structures (systems) built at the same t (Fig. 4a), we can consider one and the same structure (system) exposed to the same input at various times (Fig. 4b), provided that the age t_0 at the beginning of the exposure is the same for all cases. This is equivalent to shifting the random history of input (environment, loading) in time (Fig. 4b) relative to the instant the system is built, and considering only one and the same system (structure) built at a certain fixed time and exposed at the same age t_0.

Denote by θ the time measured, e.g., from the birth of Christ or the Big Bang. Let τ be the time when the system was built, i.e., the concrete was cast. Further, let $t = \theta - \tau$ be the age of concrete, θ_0 be the time when the system was exposed to the random stationary input (i.e., the structure was exposed to drying or loading), and $t_0 = \theta_0 - \tau$ be the age of the system (of the structure) at time θ_0 (see Fig. 4). According to the foregoing argument, we seek the dependence of the response $g(x, t, t_0 \tau)$ at a fixed age t (and a fixed location x) on the random input history $f(\theta) = f(t + \tau)$ as τ is varied (Fig. 4b).

First we need to determine the response to a single periodic component of the input, $e^{i\omega t}$, with ω being the circular frequency and i the imaginary unit. The response may be written as $e^{i\omega t} Y(\omega, x, t, t_0)$ where $Y(\omega, x, t, t_0)$ is called the frequency response function (which is complex valued). Note that this function depends separately on both t and t_0, whereas for non-aging systems it depends, in general, only on $t - t_0$ (and

if a stationary state has been reached, it is independent of $t - t_0$). Determining the dependence of Y on t and t_0 requires solving a Voltera integral equation or a system of ordinary differential equations in time [22].

The input spectrum $F(\omega)$ is defined as the Fourier transform of input $f(\theta)$:

$$f(\theta) = \frac{1}{2\pi} \int_{-\infty}^{\infty} F(\omega) e^{i\omega\theta} d\omega, \qquad F(\omega) = \int_{-\infty}^{\infty} f(\theta) e^{-i\omega\theta} d\theta \tag{23}$$

Because of linearity of the system, the Fourier transform of the general response $g(x, t, t_0, \tau)$ must then be

$$G(\omega, x, t, t_0) = F(\omega)\ Y(\omega, x, t, t_0) \tag{24}$$

The response may be expressed as the inverse Fourier transform of G(...):

$$g(x, t, t_0, \tau) = \frac{1}{2\pi} \int_{-\infty}^{\infty} G(\omega, x, t, t_0) e^{i\omega(t+\tau)} d\omega \tag{25}$$

Substitution Eq. 24 and Eq. 23 then provides

$$g(x, t, t_0, \tau) = \frac{1}{2\pi} \int_{-\infty}^{\infty} Y(\omega, x, t, t_0) e^{i\omega(t+\tau)} \int_{-\infty}^{\infty} f(\eta) e^{-i\omega\eta} d\eta\, d\omega \tag{26}$$

The second integral can be easily evaluated if $f(\eta)$ is a unit impulse at time ζ, i.e., if $f(\eta) = \delta(\eta - \zeta)$ where δ denotes Dirac delta function. Let $\xi = \theta - \zeta$ be the time lag after the impulse (Fig. 4d). The response g(...) to the impulse $f(\eta)$ is then the impulse response function $y(x, t, t_0, \xi)$. Hence, the second integral in Eq. 26 is $e^{-i\omega\zeta}$, and since $e^{i\omega\theta}\ e^{-i\omega\zeta} = e^{i\omega\xi}$, Eq. 26 reduces to

$$y(x, t, t_0, \xi) = \frac{1}{2\pi} \int_{-\infty}^{\infty} Y(\omega, x, t_0 + \xi, t_0) e^{i\omega\xi} d\omega \tag{27}$$

Thus, the impulse response function is the inverse Fourier transform of the frequency response function, same as for stationary systems. Also,

the frequency response function is the Fourier transform of the impulse response function;

$$Y(\omega, x, t, t_0) = \int_0^\infty y(x, t, t_0, \xi)\, e^{-i\omega\xi}\, d\xi \tag{28}$$

in which the lower limit of integration, $-\infty$, has been replaced by 0 because $y(x, t, t_0, \xi) = 0$ if $\xi < 0$.

The statistical properties of a stationary random process, such as $f(\theta)$, may be completely characterized by its autocorrelation function, which is defined as

$$R_f(\lambda) = \lim_{T\to\infty} \frac{1}{2T} \int_{-T}^{T} f(\theta) f(\theta + \lambda) d\theta = E\left[f(\theta) f(\theta + \lambda)\right] \tag{29}$$

in which E is the expectation. The spectral density of input $f(\theta)$ then is related to $R_f(\lambda)$ as [23-26]:

$$S_f(\omega) = \int_{-\infty}^{\infty} R_f(\lambda) e^{-i\omega\lambda}\, d\lambda \;,\; R_f(\lambda) = \frac{1}{2\pi} \int_{-\infty}^{\infty} S_f(\omega)\, e^{i\omega\lambda}\, d\omega \tag{30}$$

Let us now calculate the autocorrelation function of response at fixed age t (and at fixed t_0 and x) as τ is varied, i.e., as the input history is shifted against the instant the system is built. Since the response must be stationary with regard to τ, this function may be defined in the usual manner,

$$R_g(\lambda, x, t, t_0) = \lim_{T\to\infty} \frac{1}{2\pi} \int_{-T}^{T} g(x, t, t_0, \tau) g(x, t, t_0, \tau+\lambda) d\tau$$
$$= E[g(x, t, t_0, \tau) g(x, t, t_0, \tau+\lambda)] \tag{31}$$

Now, according to the Wiener-Khintchine relation [23], the spectral density of the response is given by the Fourier transform

$$S_g(\omega, x, t, t_0) = \int_{-\infty}^{\infty} R_g(\lambda, x, t, t_0) e^{-i\omega\lambda} d\lambda \tag{32}$$

which has the inverse

$$R_g(\lambda, x, t, t_0) = \frac{1}{2\pi} \int_{-\infty}^{\infty} S_g(\omega, x, t, t_0)\, e^{i\omega x} d\omega \tag{33}$$

The last equation is crucial. The Wiener-Khintchine relation, of course, applies only to stationary processes [23-26]. The response is nonstaionary as a function of age 5. The device that permits the use of the Wiener-Khintchine relation is to freeze the age and consider the dependence of the response at fixed t on the shift τ of the stationary input against the instant the system is built. As a function of τ, the response is stationary.

The principle of superposition now yields

$$g(x, t, t_0, \tau) = \int_0^\infty y(x, t, t_0, \xi)\, f(\tau+t-\xi) d\xi = \int_{-\infty}^{\infty} y(x, t, t_0, \xi) f(\tau+t-\xi) d\xi \tag{34}$$

where ξ is the time lag shown in Fig. 4e. The lower integration limit $-\infty$ has been replaced by 0 because the future can have no effect on the present, $y(x, t, t_0, \xi) = 0$ for $\xi < 0$. Consequently,

$$g(x, t, t_0, \tau)\; g(x, t, t_0, \tau + \lambda) = \int_{-\infty}^{\infty} y(x, t, t_0, \xi)\, f(\tau+t-\xi) d\xi \int_{-\infty}^{\infty} y(x, t, t_0, \eta)\, f(\tau+\lambda+t-\eta) d\eta \tag{35}$$

and assuming these integrals to be convergent, we obtain

$$E[g(x, t, t_0, \tau)\; g(x, t, t_0, \tau+\lambda)] = \int_{-\infty}^{\infty}\int_{-\infty}^{\infty} E[f(\tau+t-\xi) f(\tau+\lambda+t-\eta)] y(x, t, t_0, \xi) y(x, t, t_0, \eta) d\xi d\eta \tag{36}$$

Recognizing here the autocorrelation functions of the input and the response, we get

$$R_g(\lambda,x,t,t_0)=\int_{-\infty}^{\infty}\int_{-\infty}^{\infty}R_f(\xi-\eta+\lambda)y(x,t,t_0,\xi)y(x,t,t_0,\eta)d\xi d\eta \tag{37}$$

and

$$\begin{aligned}S_g(\omega,x,t,t_0) &= \int_{-\infty}^{\infty}R_g(\lambda,x,t,t_0)e^{-i\omega\lambda}d\lambda\\ &= \int_{-\infty}^{\infty}e^{-i\omega\lambda}d\lambda\int_{-\infty}^{\infty}\int_{-\infty}^{\infty}R_f(\xi-\eta+\lambda)y(x,t,t_0,\xi)y(x,t,t_0,\eta)d\xi d\eta \\ &= \int_{-\infty}^{\infty}y(x,t,t_0,\xi)e^{-i\omega\xi}d\xi\int_{-\infty}^{\infty}y(x,t,t_0,\eta)e^{-i(-\omega)\eta}d\eta\int_{-\infty}^{\infty}R_f(\xi-\eta+\lambda)e^{-i\omega(\xi-\eta+\lambda)}d\lambda\end{aligned} \tag{38}$$

The integration over λ in the last integral is at constant ξ and η. Setting $\xi - \eta + \lambda = \zeta$ and $d\lambda = d\zeta$, we recognize the last integral to be $\int_{-\infty}^{\infty}R_f(\zeta)e^{-i\omega\zeta}\,d\zeta$, which equals $S_f(\omega)$, according to Eq. 30. According to Eq. 28, the first integral in Eq. 38 is $Y(\omega,x,t,t_0)$, and the second one is $Y(-\omega,x,t,t_0)$. So we have $S_g(\omega,x,t,t_0) = Y(\omega,x,t,t_0)\ Y(-\omega,x,t,t_0)\ S_f(\omega)$. Furthermore, if $Y(\omega,\ldots) = Y_1 + iY_2$, then $Y(-\omega,\ldots) = Y_1 - iY_2$, i.e., $Y(-\omega,\ldots) = Y^*(\omega,\ldots)$ = complex conjugate of $Y(\omega,\ldots)$. $Y(\omega,..)\ Y(-\omega,..) = Y_1^2 + Y_2^2 = |Y(\omega,\ldots)|^2$. Thus, we obtain the following fundamental result

$$S_g(\omega,x,t,t_0) = |Y(\omega,x,t,t_0)|^2\ S_f(\omega) \tag{39}$$

This is the same as the classical result for stationary response of nonaging systems [23], except for the presence of arguments t and t_0. In fact, the entire derivation is similar to that used for nonaging response [23].

Note that Eq. 39, is algebraic, while the relation between the autocorrelation functions of the input and the output (Eq. 37) is given by a double integral. This represents the main advantage of the spectral approach to aging systems.

Based on Eq. 39, the mean response and the mean square response can be determined [21] in the usual manner [23]. In particular, if we split the input and the response into the mean and the deviation from the mean, i.e., $f(\theta) = \bar{f}(\theta) + \tilde{f}(\theta)$ and $g(x,t,t_0,\tau) = \bar{g}(x,t,t_0,\tau) + \tilde{g}(x,t,t_0,\tau)$, then the variance of the response may be shown [21] to be given as

$$\mathrm{Var}[g(x,t,t_0,\tau)] = \frac{1}{2\pi}\int_{-\infty}^{\infty}S_{\tilde{g}}(\omega,x,t,t_0)d\omega = \frac{1}{2\pi}\int_{-\infty}^{\infty}|Y(\omega,x,t,t_0)|^2 S_{\tilde{f}}(\omega)d\omega \tag{40}$$

For a single frequency input, i.e., $S_{\tilde{f}}(\omega) = 2\pi\ \delta(\omega - \omega_0)$ = Dirac delta function, Eq. 40 reduces to $\mathrm{Var}[\tilde{g}(\ldots)] = |Y(\omega_0,x,t,t_0)|\mathrm{Var}[\tilde{f}(\ldots)]$.

Using the spectral approach just outlined, random shrinkage stresses in a concrete half-space exposed at its surface to random environmental humidity of a given spectrum have been analyzed in Ref. 22. The age dependence of the viscoelastic properties of concrete was taken into account, and so was the age dependence of the drying diffusivity of concrete in the diffusion equation. By a certain transformation of variables, the determination of pore humidity in the half space has been reduced to the evaluation of a certain integral, which could be done numerically with a high accuracy. Complex variable expressions for the frequency response functions of pore humidity and stress components in the half space have been obtained and evaluated numerically. The dependence of these functions on the current age of concrete and on the age when drying begins has been determined. The standard deviations of pore humidity and of stress components in the half space have been calculated; they have been found to exhibit oscillations about a drifting mean. Numerical results demonstrated that, for typical diffusivity values of concrete, the solution is nonstationary for at least 50 years, for environmental fluctuations of

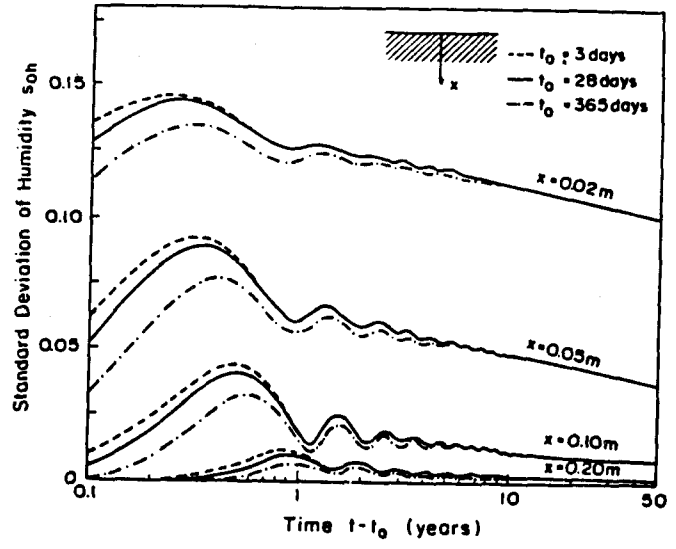

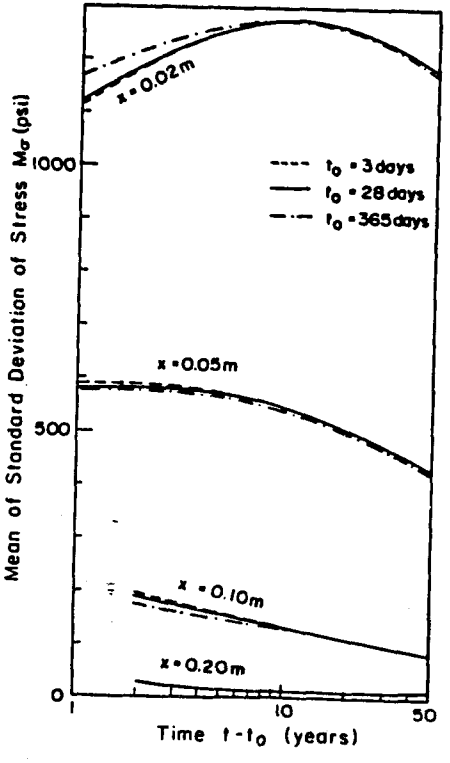

Fig. 5

Numerical Results Calculated by Bažant and Wang (1982), using the Spectral Method, for an Aging Halfspace Exposed at Surface to Humidity Oscillating with a Period 1 Year.

dominant period 1 year. For this period, the fluctuations are not felt at depths over 20 cm below the surface. The solutions have been plotted graphically [22]. In Fig. 5 we demonstrate some of the results from Ref. 22. Plotted is the standard deviation of pore humidity and of the normal stress parallel to half space surface, produced by a single frequency component of environmental humidity, with a period of 1 year. The time dependence of the standard deviations is shown for various depths below the surface and for various ages of the half space at the instant when exposure begins. The drying diffusivity is considered as $C(t) = 61\ t^{-0.213}$ mm^2/day; the creep properties are the same as those for Ross Dam concrete [1, 10], the Poisson ratio is 0.18 (independent of t and t'), and the shrinkage strain increments are 0.0016 times the pore humidity increments [22].

To analyze the long time response of an aging concrete structure subjected to random environment or random loading, the finite element approach has to be adopted. In a direct application of the foregoing analysis to a concrete structure characterized by its compliance function, one would have to evaluate numerically a vast number of history integrals over periodic components for each point of the structure and each discrete time. One can quickly realize that this approach is not feasible, even with the largest computers. To make a numerical solution possible, the exponential algorithm previously developed for the creep analysis of concrete structures under steady load has been generalized for the case of periodic loading [27]. In this approach, one first replaces the Volterra history integral defining the stress-strain relation by a rate-type stress-strain relation modeled by Maxwell chain with age dependent viscosities and elastic moduli. The first-order differential equations characterizing the

Maxwell chain are written in complex variables (complex stresses and complex strains) and their solution is obtained for time intervals for which the properties of the system may be considered as constant within the time interval. These solutions are obtained exactly and yield recurrent relations for the complex-valued stresses and strains and the complex-valued partial stresses of the Maxwell chain (internal variables). These recurrent algebraic relations may be cast in a form of an incremental elastic stress-strain relation with inelastic strains that may be evaluated in advance. These stress-strain relations are characterized by complex-valued incremental elastic moduli. Based on these moduli, one evaluates, in the usual manner, the complex-valued stiffness matrix of the structure for each time increment, and the complex-valued nodal force increments equivalent to the inelastic strains. Solving the system of finite element equations yields complex-valued increments of nodal displacements and of stresses in the finite elements. This algorithm has been programmed and applied to the analysis of a thick-wall cylindrical vessel. The results have been found to be in excellent agreement with a highly accurate solution based on the evaluation of history integrals for the case when numerical evaluation is feasible [27].

Uncertainty Analysis of Structural Effects

The spectral analysis of structural response is no doubt too sophisticated for regular design applications. The Bayesian approach to creep prediction is also intended for special structures and would not be used in regular design. For the usual creep and shrinkage analysis of creep-sensitive structures, a simpler model is needed. One such model has been recently presented by Madsen and Bažant [28]. This model yields the elementary statistics such as the mean value function and the covariance

function, including the variance function, which are of most interest for serviceability analysis. Any deterministic creep and shrinkage formula can serve as the basis for this approach. The deterministic formulas are randomized by introducing the entering parameters as random variables, and by further introducing random model uncertainty factors that characterize the incompleteness or inadequacy of the deterministic formulas. Statistics for the model uncertainty factors are derived by a comparison between available test data and predictions for these tests by the formulas. The creep and shrinkage formulas of the BP Model [1] were chosen for this purpose. For the computation of the statistics of the structural response, the method of point estimates for probability moments [29] is used. In the simplest form of this approach only two points $\mu \pm s$ need to be considered for each random variable (μ = mean of the variable, and s = its standard deviation). This approach reduces the statistical analysis to a manageable number of deterministic structural analyses for various combinations of the two values for all material parameters. The method has been demonstrated by numerous examples [28].

Concluding Remarks

Following a very rapid development of the mathematical models and experimental basis for creep and shrinkage analysis of concrete structures, which has been witnessed during the last decade, the time is now ripe to start developing probabilistically based methods, and eventually include some of them in code recommendations for practical design. As demonstrated in this paper and elsewhere, probabilistically based methods exist and are feasible, and a statistical basis for a probabilistic approach is also beginning to emerge, although much more work and refinement remains to be

done. Concrete creep and shrinkage is a highly uncertain phenomenon, with a statistical variability that is larger than that of strength. The consequences of a large error in predicting creep and shrinkage frequently greatly shorten the service life of the structure, and sometimes may even lead to catastrophic collapse, as in creep buckling or in case of detrimental effects of creep and shrinkage on other types of structural failure.

Design of concrete structures that are sensitive to creep should, therefore, be made not for the mean predictions of creep and shrinkage effects, as has been done up to now, but for extreme effects, determined on the basis of a certain, judiciously chosen confidence limit. The code-making societies would be wise to begin tackling this problem.

Acknowledgment

Partial financial support under National Science Foundation Grant No.CEE-8009050 is gratefully acknowledged. Mary Hill is to be thanked for her excellent secretarial assistance.

References

1. Bažant, Z. P., and Panula, L., "Practical Prediction of Time-Dependent Deformations of Concrete," Materials and Structures, Part I and II: Vol. 11, No. 65, 1978, pp. 307-328, Part III and IV: Vol. 11, No. 66, 1978, pp. 415-434, Parts V and VI: Vol. 12, No. 69. 1979.

2. Bažant, Z. P., and Panula, L., "Creep and Shrinkage Characterization for Prestressed Concrete Structures," J. of the Prestressed Concrete Institute, Vol. 25, 1980, pp. 86-122.

3. Zebich, S., and Bažant, Z. P., "Linear Regression Statistics of Creep and Shrinkage Data," Report No. 81-12/665s, Center for Concrete and Geomaterials, The Technological Institute, Northwestern University, Evanston, Illinois, Dec. 1981.

4. ACI Committee 209/11 (chaired by D. E. Branson, "Prediction of Creep, Shrinkage and Temperature Effecrs on Concrete Structures," ACI-SP27, Designing for Effects of Creep, Shrinkage and Temperature, American Concrete Institute, Detroit, 1971, pp. 51-93, and revised version in ACI-SP-76, Detroit, 1982, "Designing for Creep and Shrinkage in Concrete Structures (A. Pauw Symp., held at ACI Convention, Houston, 1979) pp. 193-300.

5. Tang, W. H., "Updating Reliability of Offshore Structures," Proc. of the symposium on "Probabilistic Methods in Structural Engineering" published by ASCE, Edited by Yao, T. P., pp. 139-156, Oct. 1981.

6. CEB-FIP Model Code for Concrete Structures, Committeé Eurointernational du Béton-Féderation Internationale de la Précontrainte, CEB Bulletin No. 124/125-E, Paris 1978.

7. Bažant, Z. P., and Chern, J. C., "Comment on the Use of Ross' Hyperbola and Recent Comparisons of Various Practical Creep Prediction Models," Cement and Concrete Research, Vol. 12, 1982, pp. 527-532; with discussion by Müller and Hilsdorf and reply in Vol. 13, 1983.

8. Cinlar, E., Bažant, Z. P., and Osman, E., "Stochastic Process for Extrapolating Concrete Creep," J. of the Engng. Mech. Div., Proc. ASCE, Vol. 103, 1977, 1069-1088; Disc. 1979, pp. 485-489.

9. Çinlar, E., "Probabilistic Approach to Deformations of Concrete," Chapter 3 in "Creep and Shrinkage in Concrete Structures," ed. by Z. P. Bažant and F. H. Wittmann, J. Wiley, London 1982, pp. 51-86.

10. Bažant, Z. P., "Mathematical Models for Creep and Shrinkage of Concrete," Chapter 7 in "Creep and Shrinkage in Concrete Structures," ed. by Z. P. Bažant and F. H. Wittmann, J. Wiley, London 1982, pp. 163-256.

11. Bažant. Z. P., and Chern, J. C., "Bayesian Statistical Prediction of Concrete Creep and Shrinkage," Report No. 83-4/665b, Center for Concrete and Geomaterials, Northwestern University, Apr. 1983.

12. Benjamin, J. R., and Cornell, A. C., "Probability, Statistics and Decision for Civil Engineers," McGraw Hill Book Co., New York, 1970.

13. DeGroot, M. H., "Optimal Statistical Decisions," McGraw Hill Book Co., New York, 1970.

14. Raiffa, H., and Schlaifer, R., "Applied Statistical Decision Theory," Division of Research, Graduate School of Business Administration, Harvard University, Boston, 1961.

15. Ang, A. H. S., and Tang, W. H., "Probability Concepts in Engineering Planning and Design, Vol. I - Basic Principles," John Wiley & Sons, Inc., 1975.

16. Winkler, R. L., "Introduction to Bayesian Inference and Decision," Holt, Rinehart & Winston, Inc., 1972.

17. Box, George E. P., and Tiao, George C., "Bayesian Inference in Statistical Analysis," Addison-Wesley Publishing Co., 1973.

18. McDonald, J. E., "Time-Dependent Deformation of Concrete under multiaxial Stress Conditions." Technical report C-75-4, U. S. Army Engineer Waterways Experiment Station, Vicksburg, Miss. Oct. 1975, Oak Ridge Nat'l. Lab., Oak Ridge, Tennessee 37830, Operated by Union Carbide Corp. for the U.S. Energy Research & Development Administration.

19. Heller, R. A., "Thermal Stress as a Narrow-Band Random Load," Jour. of the Eng. Mech. Division, ASCE, Vol. 102, No. EM5, Oct. 1976, pp. 787-805.

20. Tsubaki, T., and Bazant, Z. P., "Random Shrinkage Stresses in Aging Viscoelastic Vessel" Journ. of the Eng. Mech. Div., ASCE, Vol. 108, No. EM3, June 1982, pp. 527-545.

21. Bažant, Z. P., "Response of Aging Linear Systems to Random Input," Report No. 82-12/665r, Center for Concrete and Geomaterials, Northwestern University, Evanston, Illinois, Dec. 1982.

22. Bažant, Z. P., and Wang, T. S., "Spectral Analysis of Random Shrinkage in Concrete Structures," Report No. 82-12/665s, Center for Concrete and Geomaterials, Northwestern University, Evanston, Illinois, Dec. 1982.

23. Crandall, S. H., "Random Vibration in Mechanical Systems," Academic Press, New York, N. Y., 1963.

24. Fuller, W., "An Introduction to Probability Theory With Applications," 2nd Ed., Vol. 2, Chapter 19, J. Wiley & Sons, New York, 1971.

25. Newland, D. E., "An Introduction to Random Vibration and Spectral Analysis, McGraw Hill, New York, 1975.

26. Papoulis, A., "Probability, Random Variables and Stochastic Processes" McGraw-Hill, New York, 1965.

27. Bažant, Z. P., and Wang, T. S., "Complex Exponential Algorithm for Aging Creep under Random Loading," (in preparation).

28. Madsen, H. O., and Bažant, Z. P., "Uncertainty Analysis of Creep and Shrinkage Effects in Concrete Structures," ACI Journal, Vol. 80, April 1983.

29. Rosenblueth, E., "Point Estimates for Probability Moments," Proc. Nat. Academy of Sciences USA, Mathematics, Vol. 72, No. 10, pp. 3812-3814, Oct. 1975.

30. "Time Dependent Effects," Chapter 6 in "Finite Element Analysis of Reinforced Concrete," State-of-Art Report of an ASCE Structural Division Task Committee, chaired by A. Nilson, Am. Soc. of Civil Engineers, New York, 1982, pp. 309-400.